

Signal-to-noise study in low-frequency passive seismic survey
W. Yang, N. Riahi, M. Kelly

Abstract

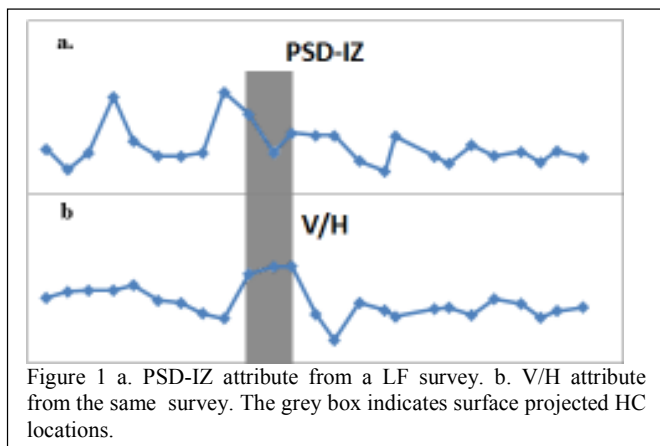
Spectral attributes of the low-frequency (LF) ambient wave field have been found to correlate with hydrocarbon (HC) reservoirs throughout the world. A major challenge today for using the LF attributes as a HC detection tool is surface wave noise. Knowing the signal-to-noise ratio (SNR) can provide insight for a better understanding of the LF phenomenon and as a guide for the noise tolerance of LF attribute based HC detection. We analyse a noisy dataset acquired in an urban area in Germany over a known oil reservoir with constrained synthetic noise models to address the SNR question in the area. Seven SNR scenarios were modeled and these synthetic datasets were used to train neural networks for HC detection. The performance of these predictors on the real dataset was used as an objective measure to estimate the SNR present in the actual data attributes. We estimate the SNR for the field data to be greater than 0.06 but less than 1.01. Based on the synthetic data alone, we estimate the minimum SNR allowable for reliable HC detection to be 0.06 for this survey. To our knowledge, this work represents a first attempt at quantitatively describing the noise tolerance of HC detection based on spectral LF features.

Introduction

Empirical evidence indicates that spectral features of the low-frequency (LF) ambient wave field are correlated with the location of hydrocarbon (HC) reservoirs (Dangel et al., 2003; Holzner et al., 2005; van Maastrigt and al Dulaijan, 2008; Lambert et al., 2008; Saenger et al., 2009). The features are usually found in the frequency band of 1-6 Hz and might be related to microtremors generated in the subsurface through an interaction of the ambient wave field with the two-phase fluid of the HC reservoir (Saenger et al., 2009). Lambert et al. (2008) and Saenger et al. (2009) describe some LF attributes that capture the low frequency anomaly. One of the major challenges for using these attributes is surface wave noise. Berteussen et al. (2009) show that surface waves energy can contaminate the LF band of interest, while Hanssen and Bussat (2007) mention the risk of confounding such energies with subsurface waves.

A noisy dataset was acquired in 2008 in an urban setting in Germany. Goertz and Schechinger (2009) analyzed the dataset with respect to the known oil reservoir using two of the LF attributes suggested by Lambert et al. (2008): PSD-IZ and V/H. While the energy attribute PSD-IZ was erratic, the spectral ratio attribute V/H did correlate with the reservoir. It can be assumed that the signal-to-noise ratio (SNR) in this dataset attribute was sufficient for HC detection. The different performance is likely the cause of the deconvolutional nature of spectral ratios.

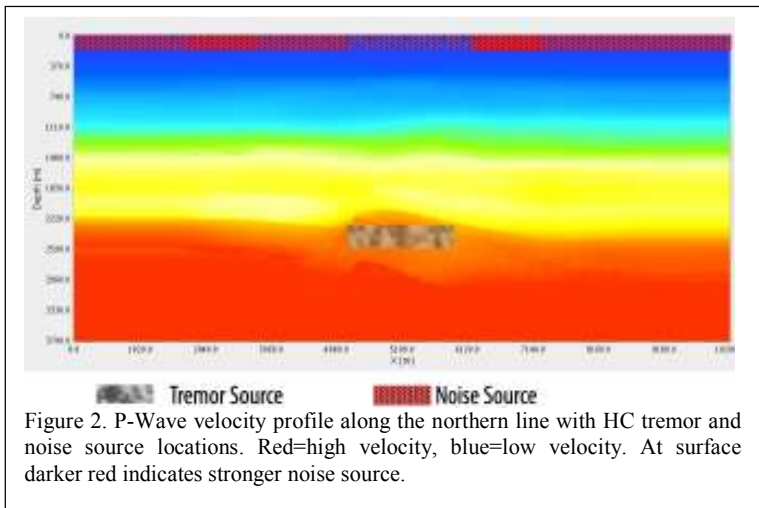
In this work we set out to estimate (1) the minimal SNR tolerance for using LF spectral attributes for HC detection and (2) the SNR level present in this survey dataset. To do so, we produced seven synthetic datasets with varying SNRs using numerical modeling. First, neural networks are trained for HC detection on these synthetic datasets, and their performance is compared with a random coin toss test to check statistical significance of detection success and establish a SNR threshold. The second agenda is addressed by applying the synthetically trained neural networks to the actual dataset. The SNR used to train the HC detector that performs best on the actual data is interpreted as being closest to representing the noise regime in the actual data.



The first section describes survey acquisition and the LF attributes used by Schechinger and Goertz (2008). Then the modeling setup is described and synthetic attribute profiles for several SNRs are shown. Both synthetic and real HC detection rates of the neural networks are given and the results are discussed.

Survey and attribute analysis

A LF survey of a 7.5 km long line consisting of 25 broadband seismometers (Nanometrics T40), spaced 300 m apart, was recorded synchronously for 48 hours over a weekend. This line crossed a known oil reservoir located approximately at its center, as well as an industrial quarter, freeways, and a major navigable waterway. The energy of the ambient wave field in this dataset is observed to be among the worlds highest in the 1 to 4 Hz band (Goertz and Schechinger, 2009). To avoid noise contamination, Goertz and Schechinger (2009) used the relatively quiet early Sunday morning time window for their analysis. They first calculated the power spectral densities (PSD) of the vertical and horizontal particle displacement. Then they computed two LF attributes: (1) PSD-IZ, the integral of the vertical PSD from 1 to 3.5 Hz, and (2) V/H, the spectra ratio of the vertical to the horizontal spectrum integrated from 1.5 to 3.5 Hz (Lambert et al., 2008). The profiles of these attributes for the line are shown in Figure 1 a,b. The PSD-IZ attribute clearly was subject to surface noise effects and fails to indicate HC reservoir locations (shown as a grey box). The V/H profile on the other hand



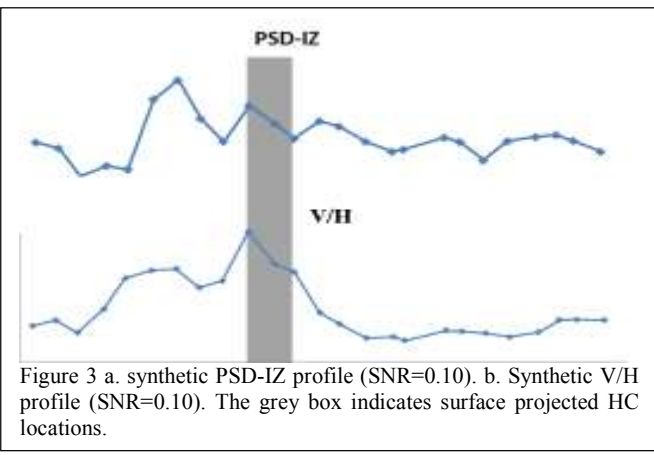
exhibits significantly higher values around the reservoir location and was thus considered to be sensitive to the subsurface oil reservoir.

Modelling Setup

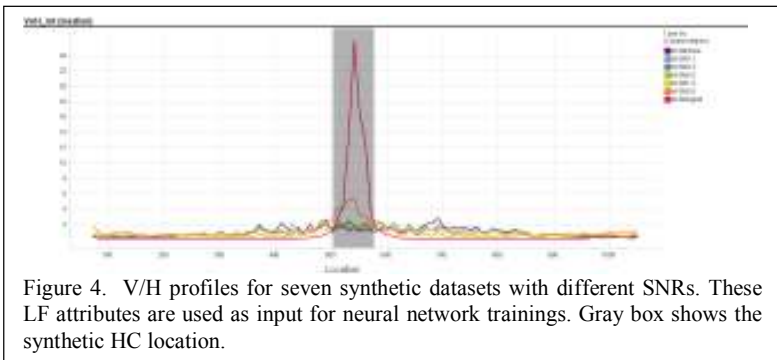
We construct an elastic model of this LF line. The model is 11.2-km long by 3.7-km deep. Figure 2 shows the P-wave velocity distribution obtained from a previous seismic 3D survey of this line. Uniform density of 2000 kg/m³ and

constant Poisson's ratio of 0.25 were used. The model is discretized into a regular grid of 10m by 10m and a staggered-grid finite difference solver (Saenger et al. 1999) is used for forward modelling.

Even though the exact source generation mechanism is unknown, here we model the reservoir as a collection of primary tremor sources consisting of horizontal line sources around 200-500m long. A vertical polarization of the sources is used because of the high V/H ratio observed at reservoir location (Goertz and Schechinger, 2009). The tremor sources consist of Ricker wavelets with a 3 Hz center frequency uniformly distributed in time. As shown in Figure 2, these sources are randomly placed in the simulation space within a 1.5 km-wide region beneath the surface which coincides with the actual reservoir location in the model domain. Surface noise sources are also modeled as primary sources. These are short line sources about 10-30 m long, with 0.1-15 Hz filtered white noise. Since we cannot assume a particular polarization of the noise, they are modeled as either vertically or horizontally polarized. Noise sources, hatched boxes at the surface in Figure 2, are placed between 0-20m depth at locations identified as major noise sources such as freeways, industrial and town centers, and major waterways. Both the vertical and horizontal particle velocities are recorded at the surface.



Seven SNR scenarios are simulated: {inf, 1.01, 0.20, 0.10, 0.06, 0.02, 0}. We define SNR as the ratio between the power density of tremor to surface noise as picked up by a (virtual) seismometer above the HC location. Infinite SNR means that there is no noise present – an unrealistic scenario. If the simulation results of this case compares well with the



actual survey result, it indicated that our numeric model is inaccurate. The other end-member, SNR=0 means no tremor signal is present. If this result compares well with the actual survey, it indicates the LF attribute features observed by Goertz and Schechinger (2009) cannot be attributed to a subsurface origin. The comparison of these synthetic results with the actual data will let us identify SNR present during this survey.

Maximum SNR threshold.

The same attributes used by Schechinger and Goertz (2009) are computed for the seven SNR synthetic datasets. PSD-IZ and V/H profiles of SNR0.10 are shown in Figure 3a and b, respectively. As in the actual survey results shown in Figure 1, the PSD-IZ profile is strongly affected by the surface noise and does not correlate with the reservoir location. Conversely, the V/H profile matches the actual profile with strongest values around the reservoir location and a low plateau at the right. The model is thus reproducing important features of the actual data set, which corroborates its use.

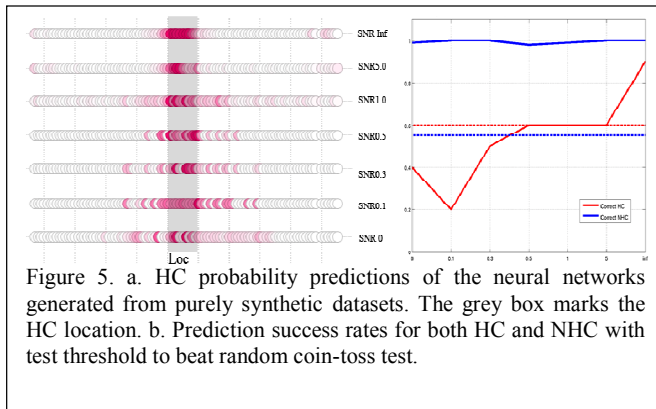


Figure 5. a. HC probability predictions of the neural networks generated from purely synthetic datasets. The grey box marks the HC location. b. Prediction success rates for both HC and NHC with test threshold to beat random coin-toss test.

Figure 4 shows the V/H profiles for the seven synthetic SNR datasets. The profiles are normalized to have a mean of 1 so they can be plotted together. These profiles are used to train seven neural networks for HC prediction, one for each SNR scenario. The neural networks are multi-layer perceptron with one hidden layer. To avoid over training each network is trained on 80% of input data, and uses the remaining 20% data for testing (see, e.g., Duda, 2001). The actual survey only contains 25 stations with 3 of them above HC reservoir. Small training samples exacerbate the issue of over training. To avoid this, we choose to use a denser spatial sampling, and 98 synthetic stations are used, with 10 of them above HC reservoirs.

We evaluate the success rate of each neural network based on (1) the fraction of correctly detected HC receivers (*true positives, TP*) and (2) the fraction of correctly detected NHC receivers, (*true negatives, TN*). Figure 5a shows the HC probability predictions for the various SNR scenarios, with the darker red circle indicating a probability of 1 for HC and white circle indicating a probability of 0. Figure 5b shows the success rates (TP and TN) plotted against the neural network SNR value. The dashed lines here indicate the maximum expected success rate of a random coin-toss prediction at significance level 80%. The neural networks trained below a SNR of 0.06 fail to beat this random predictor and are considered not statistically significant. Based on the synthetic data we thus establish a minimum required SNR at which the spectral V/H attribute can be used for HC detection here.

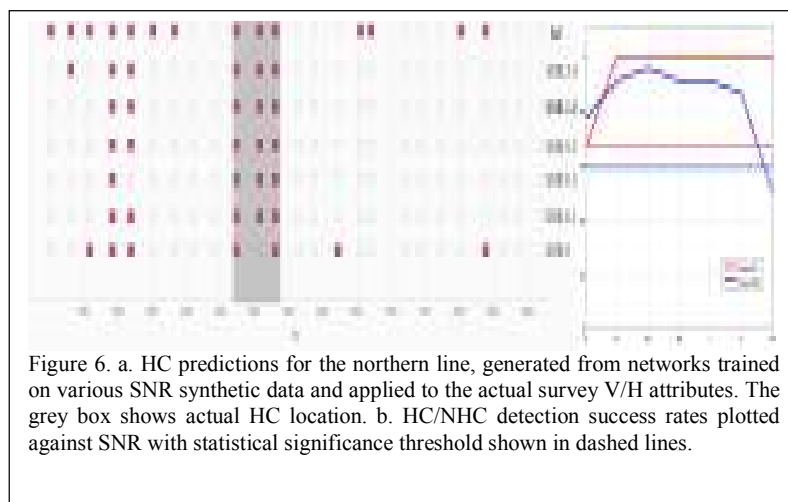


Figure 6. a. HC predictions for the northern line, generated from networks trained on various SNR synthetic data and applied to the actual survey V/H attributes. The grey box shows actual HC location. b. HC/NHC detection success rates plotted against SNR with statistical significance threshold shown in dashed lines.

SNR Estimation of the Survey Data

We applied the seven neural networks on the actual V/H profile of Goertz and Schechinger (2009). Again, prediction profiles and success rates are calculated and shown in figures 6 a,b. As expected the SNR 0 predictor fails, but also the infinite SNR predictor fails as well. We discard the predictions made by neural

networks with $SNR \leq 0.06$, since they do not beat the coin-toss test threshold. The remaining three SNR predictors all correctly identified the HC stations. However, SNR 1.01 predictor miss identifies three NHC stations, one extra miss identification than the two miss identifications made by SNR 0.20 and 0.10 predictor. From this performance, we thus estimate that the SNR in this data set is less than 1.01 but greater than 0.06.

Conclusion

The predictors trained on $SNR \leq 0.06$ fail to beat the uninformed coin-toss test in predicting the synthetic HC locations. For a reliable HC detection using the spectral V/H attribute we therefore conclude that the SNR has to be above 0.06 for the particular configuration we studied.

Since neither of the extreme cases, $SNR=0$ or infinite, provide a good match to actual survey data, we conclude that there are both surface noise and subsurface signal present in this survey. Based on the performance of the HC and NHC predictions made on the other SNR models we estimate that the effective signal-to-noise regime here falls somewhere between 0.06 to 1.01 (linear scale). The underperformance of other neural networks, the extreme cases and SNR1.01, are due to using a predictor that was trained in a wrong SNR regime and therefore can not interpret the data correctly.

Reference:

Dangel, S., Schaepman, M.E., Stoll, E.P., Carniel, R., Barzandji, O., Rode, E.-D., and Singer J.M. [2003] Phenomenology of tremor-like signals observed over hydrocarbon reservoirs. *Journal of Volcanology and Geothermal Research*

Holzner, R., Eschle, P., Zürcher, H., Lambert, M., Graf, R., Dangel, S. and Meier P. F. [2005] Applying microtremor analysis to identify hydrocarbon reservoirs. *First Break*, 23

van Mastriigt, P. and Al-Dulaijan, A. [2008] Seismic Spectroscopy Using Amplified 3C Geophones. 70th EAGE Conference & Exhibition, expanded abstracts

Lambert, M., Schmalholz, S. M., Saenger, E. H. and Steiner, B. [2008] Low-frequency microtremor anomalies at an oil and gas field in Voitsdorf, Austria. *Geophysical Prospecting*, 0, 1-19

Saenger, E. H., Schmalholz, S. M., Lambert, M., Nguyen, T. T., Torres, A., Metzger, S., Habiger, R. M., Müller, T., Rentsch, S. and Mendez-Hernandez, E. [2009] A passive seismic survey over a gas field: analysis of low-frequency anomalies. *Geophysics* vol. 74

Ali, M. Y., Berteussen, K. A., Small, J., Anjana, B.T., Barkat, B. and Pahlevi, O. [2009] Recent Low Frequency Passive Seismic Experiments in Abu Dhabi. 71st EAGE Conference & Exhibition, expanded abstracts

Hanssen P. and Bussat S. [2008] Pitfalls in the analysis of low frequency passive seismic data. *First Break* vol. 26

Goertz, A., Schechinger, B., Koerbe, M. and Krajewski, P. [2009] A Low-Frequency Passive Seismic Survey in an Urban Setting in Germany. 71st EAGE Conference & Exhibition, expanded abstracts

Sanger, E. H., Gold, N. and Shapiro, S. A. [1999] Modeling of elastic waves in fractured media using the rotated staggered finite-difference grid. 69th SEG Conference and Exhibition, expanded abstracts

Duda, R. O., Hart, P. E. and Stork, D. G. [2001] *Pattern Classification*, John Wiley & Sons, 2nd ed.